論文 An Analysis of the Influence of Bond Conditions of Tendons on the Hysteretic Behavior of PC Members

Chengxu YANG[*1], Hitoshi SHIOHARA[*2] and Shunsuke OTANI[*3]

ABSTRACT

Prestressed concrete (PC) members and reinforced concrete (RC) members show different hysteretic loops under cyclic loading. One of the reasons may be the different bond condition of tendons in PC members. An analytical model considering bond-slip of tendons was developed by the authors and was applied to PC beams. The influence of the bond conditions on hysteretic behavior was investigated. The bond strength of the tendons was found to be the most influential on hysteretic behavior of PC members. Beams with high bond strength are predicted to possess satisfactory hysteretic behaviors comparable to RC beams with sound bond.

KEYWORDS: Prestressed Concrete, Hysteretic Behavior, Bond-Slip, Nonlinear Analysis

1. INTRODUCTION

Prestressed concrete (PC) members have hysteretic loops with a shape of an "S" and their energy dissipation is smaller than that of reinforced concrete (RC) members. The reasons may include difference between the material properties of reinforcement bars and tendons, the presence of the prestress, and the different bond conditions of the reinforcement bars and tendons. Adachi et al. [1] made an analytical investigation on the influence of bond conditions of tendons on the hysteretic behavior of PC members, adopting Kosaka's analytical model[2]. The authors proposed a new analytical model [3,4], considering bond-slip relation of tendons. The model is based on the division of a member on both longitudinal and transverse directions like Kosaka's model. However a virtual rigid constraint was introduced where the bond-slip between the tendons and concrete is assumed to occur solely on the nodes and the equations of equilibrium and deformation consistency are set up on the level of a section. Compared with Kosaka's model and FEM approaches, the model is simpler and the analysis effort is comparatively small. By using this model, an analysis was conducted on a cyclically loaded PC specimen. The effects of stiffness and strength of the bond-slip relation are investigated in this report.

2. ANALYTICAL MODEL

2.1 ASSUMPTIONS

The model [3,4] employed in this study is shown in Fig. 1. A member is divided into a finite number of segments in the longitudinal direction along the central axis of the member. In the transverse direction, each segment is divided into a finite number of layers that are represented by the same number of concrete springs like the fiber model. Each level of reinforcing bars in the segment was represented by a bar spring. All of these springs and rigid joints represent the reinforced concrete part, to which the "plane section assumption" is applicable. Between the two adjacent segments is a

*1 Department of Architecture, Graduate School of Engineering, University of Tokyo, PhD Candidate, Member of JCI
*2 Department of Architecture, School of Engineering, University of Tokyo, Associate Professor, Dr.Eng, Member of JCI
*3 Department of Architecture, School of Engineering, University of Tokyo, Professor, PhD, Member of JCI

virtual rigid constraint to which the springs of concrete and reinforcing bars are fixed. The tendons in the segment are also represented by the same number of springs that are connected to the rigid constraints indirectly, through the bond-slip springs. One end of the bond-slip spring is connected to the end of a tendon and the other end of the bond-slip spring is connected to a rigid constraint. Bond is assumed to occur only between the ends of the tendons and the rigid constraint. For convenience, the number of the tendons is assumed to be two in this paper. In the middle of the segment, there is a combination of a "slide-free" device, a pin and a shear spring for transmitting the shear force only.

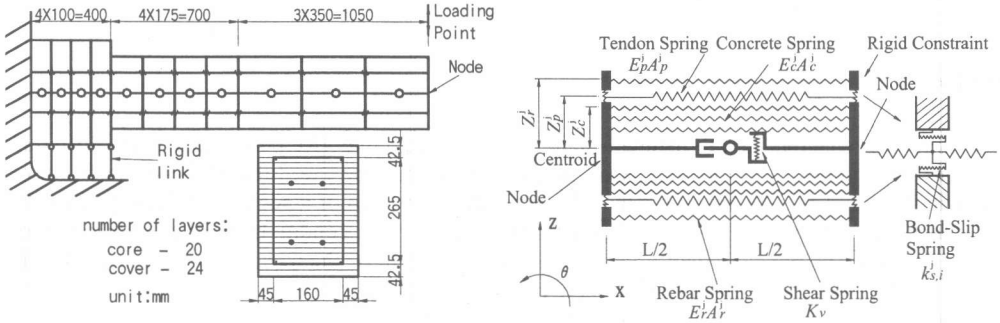

(1) Division of member and section **(2) Springs of a segment**

Fig. 1 Analytical model

Each node have five independent degrees of freedom: three for the RC part (the displacements in X, Z directions and the rotation angle θ) and two for the tendons (the displacement in X direction only, one for each tendon).

2.2 FORMATION OF STIFFNESS MATRIX OF EACH SEGMENT

For the RC part, the relation between the end forces $\{\Delta P\}$ and end displacements $\{\Delta D\}$ of the i-th segment can be expressed by

$$\{\Delta P\}_i^{rc} = [K]_i^{rc}\{\Delta D\}_i^{rc} \tag{1}$$

$$\{\Delta P\}_i^{rc} = \left\{\{\Delta P_1\}^T \mid \{\Delta P_2\}^T\right\}_i^T = \{\Delta P_{x1}\ \Delta P_{z1}\ \Delta M_1 \mid \Delta P_{x2}\ \Delta P_{z2}\ \Delta M_2\}_i^T \tag{2}$$

$$\{\Delta D\}_i^{rc} = \left\{\{\Delta D_1\}^T \mid \{\Delta D_2\}^T\right\}_i^T = \{\Delta D_{x1}\ \Delta D_{z1}\ \Delta\theta_1 \mid \Delta D_{x2}\ \Delta D_{z2}\ \Delta\theta_2\}_i^T \tag{3}$$

$$[K]_i^{rc} = \left[\begin{array}{c|c} K_{11} & K_{12} \\ \hline K_{21} & K_{22} \end{array}\right]_i^{rc} = \left[\begin{array}{ccc|ccc} \sum\frac{E_jA_j}{L} & 0 & -\sum\frac{E_jA_j}{L}Z_j & -\sum\frac{E_jA_j}{L} & 0 & \sum\frac{E_jA_j}{L}Z_j \\ 0 & K_v & K_v\cdot\frac{L}{2} & 0 & -K_v & K_v\cdot\frac{L}{2} \\ -\sum\frac{E_jA_j}{L}Z_j & K_v\cdot\frac{L}{2} & \sum\frac{E_jA_j}{L}Z_j^2+K_v\cdot\frac{L^2}{4} & \sum\frac{E_jA_j}{L}Z_j & -K_v\cdot\frac{L}{2} & -\sum\frac{E_jA_j}{L}Z_j^2+K_v\cdot\frac{L^2}{4} \\ \hline -\sum\frac{E_jA_j}{L} & 0 & \sum\frac{E_jA_j}{L}Z_j & \sum\frac{E_jA_j}{L} & 0 & -\sum\frac{E_jA_j}{L}Z_j \\ 0 & -K_v & -K_v\cdot\frac{L}{2} & 0 & K_v & -K_v\cdot\frac{L}{2} \\ \sum\frac{E_jA_j}{L}Z_j & K_v\cdot\frac{L}{2} & -\sum\frac{E_jA_j}{L}Z_j^2+K_v\cdot\frac{L^2}{4} & -\sum\frac{E_jA_j}{L}Z_j & -K_v\cdot\frac{L}{2} & \sum\frac{E_jA_j}{L}Z_j^2+K_v\cdot\frac{L^2}{4} \end{array}\right]_i \tag{4}$$

where, L: length of the segment, E_j: Young's module of concrete or steel, A_j: area of each concrete layer and each level of reinforcing bar, Z_j: position of each layer in height direction of each concrete layer or each level of reinforcing bar, K_v: shear stiffness (Because shear deformation is not considered, herein it is assigned a large value <10^9kN/m>.)

For the j-th tendon, the relation between the end forces $\{\Delta P\}=\{\Delta P_1^j, \Delta P_2^j\}^T$ and end displacements $\{\Delta D\}=\{\Delta D_1^j, \Delta D_2^j\}^T$ of the i-th segment can be expressed by

$$\begin{Bmatrix} \Delta P_1^j \\ \Delta P_2^j \end{Bmatrix}_i^p = \frac{E_p^j A_p^j}{L} \left[\begin{array}{c|c} 1 & -1 \\ \hline -1 & 1 \end{array}\right]_i \begin{Bmatrix} \Delta D_1^j \\ \Delta D_2^j \end{Bmatrix}_i^p \tag{5}$$

where, E_p^j: Young's module of the tendon, A_p^j: area of the tendon

2.3 EQUATIONS OF EQUILIBRIUM AT NODES

Considering the equilibrium at the i-th node of two adjacent segments shown in Fig. 2, the equations of equilibrium can be written as eqs. 6-8.

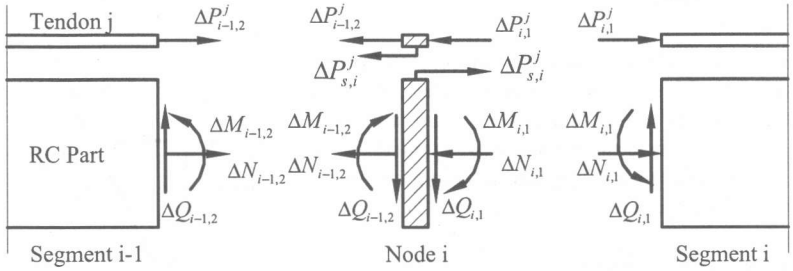

Fig. 2 Equilibrium condition at nodes

For the RC part, the equations of equilibrium of forces and moments are,

$$\Delta N_{e,i} = \Delta N_{2,i-1} + \Delta N_{1,i} - \sum_j \Delta P_{s,i}^j \tag{6}$$

$$\Delta M_{e,i} = \Delta M_{1,i-1} + \Delta M_{2,i} + \sum_j \Delta P_{s,i}^j Z_p^j \tag{7}$$

For the j-th tendon, the equation of equilibrium of forces is,

$$\Delta P_{e,i}^j = \Delta P_{2,i-1}^j + \Delta P_{1,i}^j - \Delta P_{s,i}^j \tag{8}$$

where, $\Delta N_{e,i}$ $\Delta M_{e,i}$: external nodal forces at the node (not shown in Fig. 2), $\Delta N_{k,i}$, $\Delta M_{k,i}$, $\Delta Q_{k,i}$: resultant forces of the RC part at k end (k = 1, 2) of segment i, $\Delta P_{s,i}^j$: bond force between the tendon j and the rigid joint at node i, Z_p^j : the position of the tendon in height direction.

The value of $\Delta P_{s,i}^j$ can be calculated from the relative displacement between the tendon and the rigid joint by eq. 9.

$$\Delta P_{s,i}^j = k_{s,i}^j \left[\Delta D_i^j - (\Delta D_{x,i} - \Delta\theta_i \cdot Z_p^j)\right] \tag{9}$$

where, k_{si}^j is the stiffness of bond-slip spring of the j-th tendon.

Substituting eq. 9 to eqs. 6-8, the relation between the node forces and node displacements can be derived. The total stiffness matrix of the member can be formed by a set of eqs. 10-13.

$$\{\Delta P_e\}_i^{rc} = [K_{21}]_{i-1}^{rc}\{\Delta D\}_{i-1}^{rc} + ([K_{22}]_{i-1}^{rc} + [K_{11}]_i^{rc})\{\Delta D\}_i^{rc} + [K_{12}]_i^{rc}\{\Delta D\}_{i+1}^{rc} + [C]_i\{\Delta D\}_i \quad (10)$$

$$\{\Delta P_e\}_i^{p} = [K_{21}]_{i-1}^{p}\{\Delta D\}_{i-1}^{p} + ([K_{22}]_{i-1}^{p} + [K_{11}]_i^{p})\{\Delta D\}_i^{p} + [B]_i\{\Delta D\}_i \quad (11)$$

where, $[K_{kl}]_i$: the submatrices (k,l = 1,2) of the RC part or tendons' stiffness matrix at segment i. $\{\Delta P_e\}_i$ and $\{\Delta D\}_i$: the external load and displacement vectors of node i. The superscripts rc and p show which part of the matrices or vectors they belong to. $[B]_i$ and $[C]_i$ are intermediate matrices defined by eqs. 12,13.

$$[B]_i = \begin{bmatrix} -k_{s,i}^1 & 0 & Z_p^1 \cdot k_{s,i}^1 & k_{s,i}^1 & 0 \\ -k_{s,i}^2 & 0 & Z_p^2 \cdot k_{s,i}^2 & 0 & k_{s,i}^2 \end{bmatrix} \quad (12)$$

$$[C]_i = \begin{bmatrix} -1 & -1 \\ 0 & 0 \\ Z_p^1 & Z_p^2 \end{bmatrix} [B]_i \quad (13)$$

2.4 MATERIAL MODEL

The constitutive models of concrete, reinforcing bars and tendons are the same as the models used in references [3,4]. Different model factors were assigned to core and cover concrete. A trilinear skeleton curve was applied to the bond-slip model. For the unloading and reloading curves, the bond-slip rules of Morita [5] were adopted (Fig. 3).

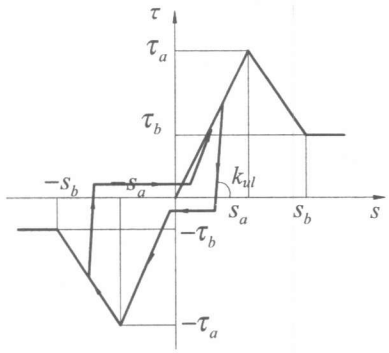

Fig.3 Bond-Slip Model (by Morita [5])

3. ANALYTICAL SPECIMENS

Sugimoto et al. conducted a cyclic loading test of PC and PRC members in 1996. One of their specimens, *L10C*, a PC cantilever beam, was selected for the analysis. The details of the specimen were reported in reference [6]. The division of the beam was shown in Fig. 1. It was divided into eleven segments in the longitudinal direction. In the direction of the beam height, the section was divided into twenty and twenty-four layers for the core and cover part, respectively. Fig. 1 also showed the support condition, by which the bond-slip of the tendons in the stub can be included.

4. ANALYTICAL RESULTS

Table 1 Bond-slip model factors

case	τ_a (MPa)	s_a (mm)	τ_b (MPa)	s_b (mm)	k_{ul} (N/mm^3)
A	2.5	0.05	0.5	0.25	400
B	25	0.50	25	1.00	400
C	25	0.05	50	0.1	400
D	0.1	0.05	0.02	0.1	40

To calculate the nonlinear response, the procedure of displacement incremental iteration in reference [3], was adopted. In the vicinity of the peaks, the size of the displacement increment was set to 0.1mm, and for other locations it was set to 0.25mm. The factors required by material model of the reinforcing bar, concrete and tendons were determined from the material test results, which can be found in reference [6].

The sole variable of the analysis was the bond-slip parameters listed in Table 1. Four cases (A-D) of analysis were carried out by altering the initial stiffness and the bond strength. Case A is

intended to simulate the realistic bond-slip parameters of the specimen. The initial stiffness of Case B is the same as Case A, whereas the bond strength is ten times larger. Case C has the same strength as Case B, while the initial stiffness is ten times larger. The bond-slip relation stays in the linear elastic range in Case C. Case D has a very small initial stiffness and bond strength almost equivalent to an unbonded condition. A common loading history, which was edited from the actual one used in the test, was taken for all four cases.

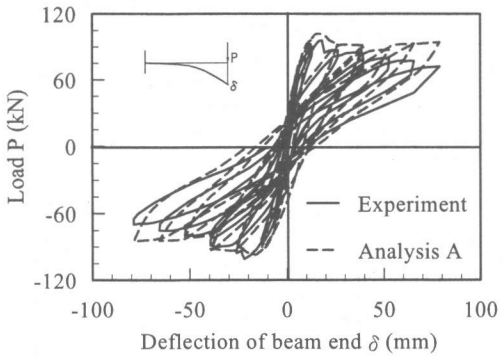

Fig. 4 Comparison of Load-Deflection relation of case A and Experiment

The comparison of the load-deflection relation of analysis case A and the experiment is shown in Fig. 4. The maximum resistance, the initial stiffness and the stiffness at maximum load show the same level of values. As deflections increase, both show a degradation of the resistance. This may result from the compressive softening of the concrete. The shape of the hysteretic loops is similar and both dissipate little energy. The difference may come from the bond-slip model of the tendons, whose factors have to be arbitrarily determined due to the scarcity of the solid experimental evidence.

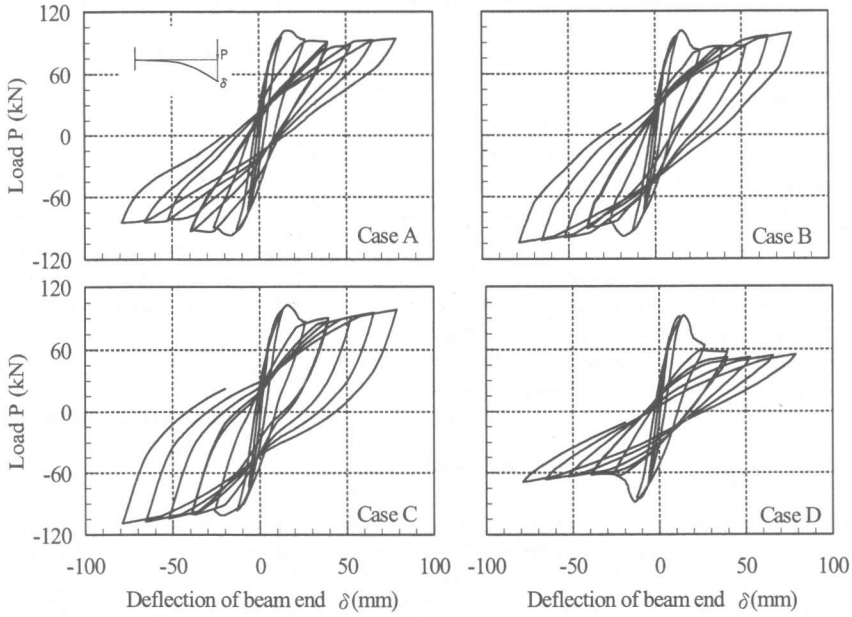

Fig. 5 Load-deflection relation of the four analytical cases

The load-deflection relations of each of the four cases are shown in Fig. 5. The shapes of hysteretic loops are significantly different. Despite the fact that the initial bond-slip stiffnesses of cases A and B are the same, the area enclosed in each cycle of case B is significantly greater than that of the corresponding cycle of case A. And the shape of the loops of case B is similar to that of RC members, whose hysteretic loops usually have a shape of a spindle. Hence the bond strength of a bond-slip spring seems to have a large impact on the hysteretic characteristics of PC members. Case C shows a fat spindle shape. Case D shows extremely small loop areas and low strength. Therefore, the

properties of bond-slip of tendons are one of the most primary factors in determining the shape of a hysteretic loop.

The equivalent damping ratios H_{eq} of all the cases are shown in Fig. 6. In cases B and C, which has large bond strengths, the values of H_{eq} increase with the increasing deformation. In case A, which has realistic bond strength, the value of H_{eq} tends to remain constant. The test shows the same result. In case D, whose bond strength is almost zero, H_{eq} value keeps declining. At large deformations, cases B and C have the largest H_{eq} values and the other cases' H_{eq} values seem to be in the same level.

The calculated strain distribution along one of the top tendons at displacement 26.3mm is shown in Fig. 7. Although Case A showed good agreement with the test in load deflection relation, the distribution pattern is quite different. Cases A and B have their largest strains occurring at the critical section, and the value of case B is greater than A. Case D has a uniform distribution of rather small strains. The test result falls between case A and case D. It seems that the bond deterioration of the tendon occurred at early loading stage.

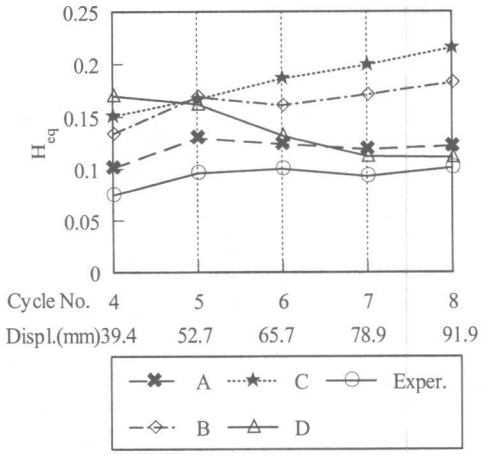

Fig.6 Equivalent damping ratio of H_{eq}

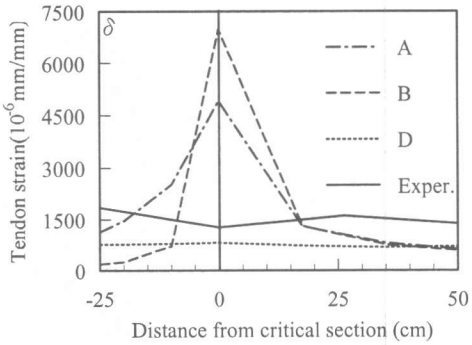

Fig.7 Strain distribution in a tendon

5. CONCLUSIONS

The conclusions can be collected as below:

(1) The model proposed by the authors was successful in simulating the hysteretic behavior of PC members.

(2) The bond-slip properties of tendons are the primarily influential factors in determining the hysteretic characteristics of PC members. Those with high bond strength show satisfactory hysteretic loop shapes comparable to RC members with sound bond.

REFERENCES

1. M. Adachi and M Nishiyama, "Hysteretic Behavior Analysis of Prestressed Concrete Assemblages Considering Bond-Slip Characteristic between Prestressing Steel and Concrete", Proceedings of the Japan Concrete Institute (1999), Vol. 21, No. 2, pp.895-900
2. Y. Yoshio, Y. Tanigawa and K. Yamada, "Inelastic analysis of Reinforced Concrete Based on Endochronic Theory", Transactions of the Architectural Institute of Japan, No.326, April 1983, pp79-90
3. C. Yang, H. Shiohara and S. Otani, "A Nonlinear Analysis of PRC members Considering Bond-Slip Conditions of Tendons", Proceedings of AIJ Annual Convention (1998), pp.1029-1030
4. H. Aono, C. Yang, H. Shiohara and S. Otani, "Nonlinear Analysis of PC Columns Simulating Bond-Slippage Property between Tendons and Concrete", Proceedings of AIJ Annual Convention (1999), pp.1049-1050
5. S. Morita and T. Kaku, "Slippage of Reinforcement in Beam-Column Joint of RC Frame", Proceedings, Eighth World Conference on Earthquake Engineering, San Francisco, July 1984, Vol. 6, pp. 477-484
6. H. Itoh, K. Sugimoto, H. Shiohara and S. Otani, "An Experimental Study on Cyclic Loads of PC Beams", Proceedings of Japan Concrete Institute (1997), Vol. 19, No. 2, pp.1137-1142